IOP Conf. Series: Materials Science and Engineering **194** (2017) 012015 doi:10.1088/1757-899X/194/1/012015

Dynamic strain aging precipitation of $Mg_{17}Al_{12}$ in AZ80 magnesium alloy during multi-directional forging process

Q F Zhu[1, 2*],G S Wang[1, 2], X J Wang[1, 2], F Z Liu[1, 2], C Y Ban[1, 2], J Z Cui[1, 2]

[1] Key Laboratory of Electromagnetic Processing of Materials, Ministry of Education, Northeastern University, Shenyang, P.R. China
[2] School of Materials Science and Engineering, Northeastern University, Shenyang, P.R. China

E-mail：zhuqingfeng@epm.neu.edu.cn

Abstract. Dynamic aging precipitation of $Mg_{17}Al_{12}$ phases in AZ80 magnesium alloy was studied by multi-directional forging (MDF) with decreasing temperatures from 410 to 300 ℃. The results show that the morphology of the dynamically precipitated β-$Mg_{17}Al_{12}$ phases (formed during forging process) exhibited granular shape. During the multi-directional forging process, the inhomogeneous dynamic precipitation of the β-$Mg_{17}Al_{12}$ phases result in the coexistence of the fine grains (with many granular $Mg_{17}Al_{12}$ phases) and coarse grains (without $Mg_{17}Al_{12}$ phases) in the samples. The fine grains (with many granular $Mg_{17}Al_{12}$ phases) area expands with the decreasing of final forging temperature. The inhomogenous Al content distribution in the Mg matrix leads to the non-uniform dynamic precipitation of the $Mg_{17}Al_{12}$ phase. These $Mg_{17}Al_{12}$ phase retards the growth of the DRX grains, which in turns results in the formation fine grains area during the during the MDF process with temperature decreasing.

1. Introduction

Dynamic strain aging (DSA) is a phenomenon in metals and alloys resulted from the interaction between the diffusing solute atoms and the moving dislocation. It has been found that DSA occurs in many alloys during uniaxial tension or compression process [1-5]. In traditional metal forming process, such as extrusion and rolling, it is difficult to control the DSA process because of the limited deformation time and deformation reduction. By contrast, the DSA process can be effectively controlled during the Sever Plastic Deformation (SPD) by constantly increasing accumulative strains. In recent years, the DSA behavior during SPD process has been widely studied [6-12]. Roven et. al [7] found that the globular β″ phase with size about 4 nm precipitated in 6063 aluminum alloy during Equal Channel Angular Pressing (ECAP) at room temperature and 175 ℃. Xia, Nie et. al [9] have studied the DSA process in magnesium alloys during the Multi-Directional Forging (MDF) process. The granular $Mg_{17}Al_{12}$ phases, which distributed along the grains boundaries, restricted the growth of dynamic recrystallized grains and therefore refined the grains. We have also found the dynamic precipitation behavior in AZ80 magnesium alloy during multi-directional forging process [12]. In this paper, dynamic strain aging precipitation of $Mg_{17}Al_{12}$ phases in the AZ80 magnesium alloy was studied by multi-directional forging (MDF) in the temperature range from 410 to 300 ℃.

2. Experimental

Rectangular samples with the size of 61 mm (z axis) × 52 mm (y axis) × 45 mm (x axis)) were cut from a commercial direct chill (DC) casting AZ80 magnesium alloy (annealed at 410 ℃ for 16 hours) with compositions of Al (7.85wt.%), Zn (0.43wt.%), Mn (0.21wt.%) and the balance Mg. The samples were heated at 410 ℃ for 1.5 hours, and then forged by a 300 t hydraulic press. Fig. 1 schematically shows the MDF process. First, the sample was forged down along the Z direction (the long side) to 35 mm (pass 1); then the sample was turned 90° around the X axis and forged down along the Y direction (newly formed long side) to 35 mm (pass 2); subsequently the sample was turned 90 ° around the Z axis and forged along the X direction to 35 mm (pass 3). The strain rate and the true strain of each pass were 0.13 s-1 and 0.5, respectively. The final forging temperature is controlled by time interval of each passes and the temperature of the forging hammers. The temperature of the samples were detected the thermocouple and thermometer. The detailed experimental parameters are shown in Table 1. Small specimens were cut from these samples. With a further grounding, polishing and oxidizing, these specimens were observed by a OM and SEM. The Al and Zn compositions in the primary Mg matrix were manually detected by the EPMA-1600/1610 Electron Probe Microanalysis (EPMA).

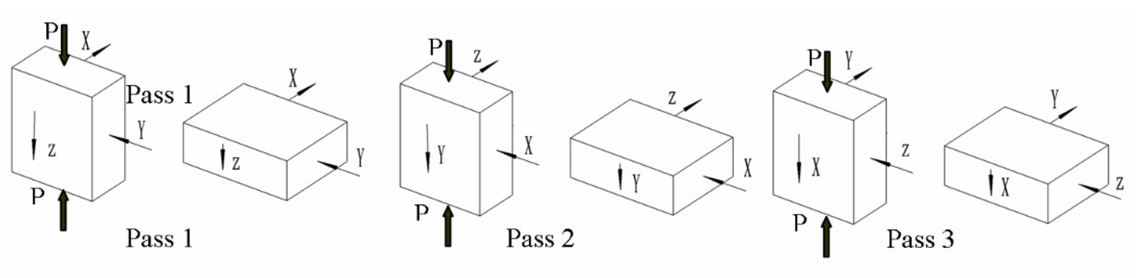

Fig. 1 Schematic diagram of the multi-directional forging

The differential scanning calorimetry (DSC) technique was employed to analysis the thermal behaviors of the AZ80 alloy. Disc-shaped sample of average weight of ～24 mg was placed in one of the pans and the aluminum reference was kept in other pan. The heating rate was 5 ℃/min. Scans were performed between room temperature and 400 ℃ in purified nitrogen flow at a rate of 50 ml min^{-1}.

Table 1. Experimental parameters

Sample number	Forging passes	Final forging temperature (℃)	Accumulative true strain (ε)
P1	4	335	2
P2	7	325	3.5
P3	14	300	7

3. Results and discussion

Fig. 2(a) shows the optical micrograph of the initial DC casting AZ80 alloy after homogenization heat treatment. It can be seen that the dendritic microstructure disappears to be replaced by the equiaxed grain. And the average grain size is about 210 μm. And some black contamination like substances are distributed along the grains boundaries. A further observation shows that these substances are composed of laminar second phase, as shown in SEM figure in Fig. 1(b). EDX analysis indicates that the phase is laminar β-$Mg_{17}Al_{12}$. A statistical measurement suggests that the mean area fraction of $Mg_{17}Al_{12}$ in the specimen is about 13.6%.

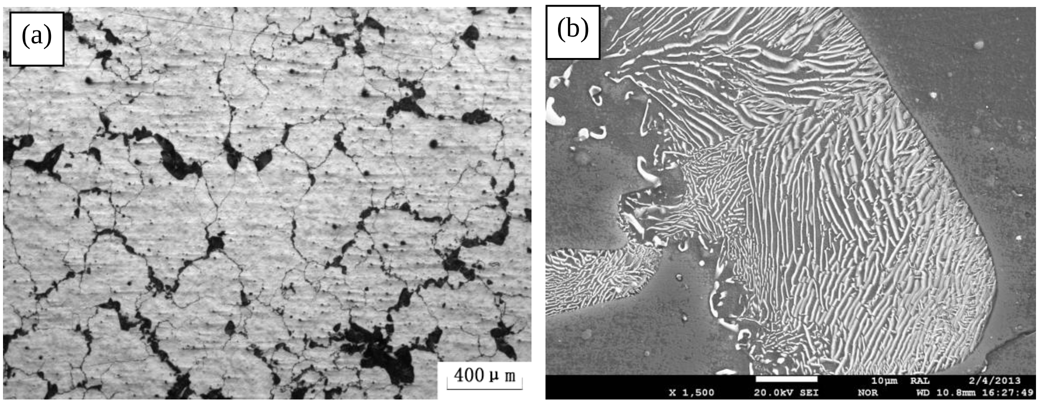

Fig.2 Microstructure of as-homogenized AZ80 alloy specimen, (a) Optical microscope images (b) magnified micrographs observed by SEM

Fig. 3 shows photography of the samples forged by different condition. It can be seen that the samples show similar outline dimensions and are generally consistent with the initial shape. There are no obvious crack and overlaps on the surface of these samples. This indicates that deformability of AZ80 sample can ensure the MDF process performed successfully.

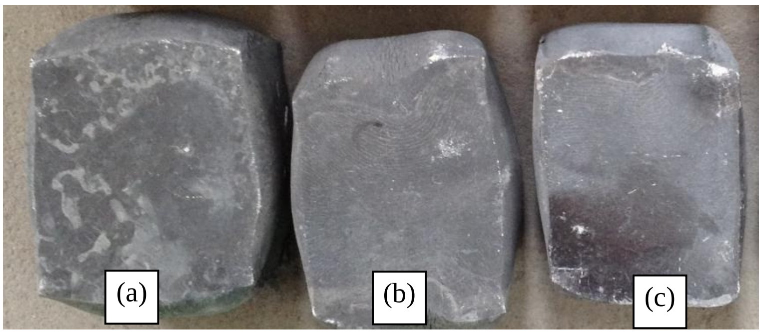

Fig. 3 Photography of the samples forged by different condition, (a) P1-sample, (b) P2-sample and (c) P3-sample

The microstructures in the center of the forged samples are displayed in Fig. 4(a)-(c).It can be found that some mutual-mixed black and white structures distribute on the center of the samples. And the areas of the black structures increase with increasing the accumulative strains and decreasing temperature. The enlarged picture shows that the black structures are very fine grains with granular second-phase β-$Mg_{17}Al_{12}$ distributed along the grain boundaries. While, the white structures are relatively coarse-grains without second-phase β-$Mg_{17}Al_{12}$ formed.

In order to reveal the details of the coarse and fine grains areas, the EPMA were employed and the intersection area of coarse and fine grains were observed and analyzed. Fig.5 (a) shows the SEM picture in the intersection area of coarse and fine grain. The left side and right side of the picture present the typical fine grain area (with granular β-$Mg_{17}Al_{12}$) and the coarse grain area, respectively. It is shown that the grain size of the AZ80 alloy gradually gets bigger, and the amount of the granular β-$Mg_{17}Al_{12}$ gradually decreases from the left to the right on Fig. (a). And the granular β-$Mg_{17}Al_{12}$ phases mainly distribute along the grain boundary of the fine grain. The element distribution along the straight line in Fig (a) is shown in Fig 5(b). It is clearly show that the wave crest of the Al element correspond with the wave valley of the Mg element on the point of granular β-$Mg_{17}Al_{12}$ phases. The wave crest of the Al mainly appears on the left of the figure, and no wave crest appears on the right of the figure. The content of the Mg element increases gradually from the left to the right. On the contrary, the content of the Al element decreases gradually from the left to the right.

Fig. 6 presents the DSC scan obtained at a heating rate of 5 ℃/min for AZ80 alloy. The DSC curve shows that an endothermic peak forms between 300 ℃ and 350 ℃. This reaction can be ascribed to the dissolution of β-$Mg_{17}Al_{12}$ phases. The Al element will precipitate from the Mg matrix as the temperature lower than 330 ℃ for this alloy. So the granular β-$Mg_{17}Al_{12}$ phases began to dynamically precipitate from the Mg matrix with the forging temperature constantly decrease from 410 ℃ to 335 ℃, as show in Fig.4 a. With the final forging temperature further decreasing to 300 ℃, more granular β-$Mg_{17}Al_{12}$ phases dynamically precipitated from the Mg matrix, as shown in Fig.4 b and c.

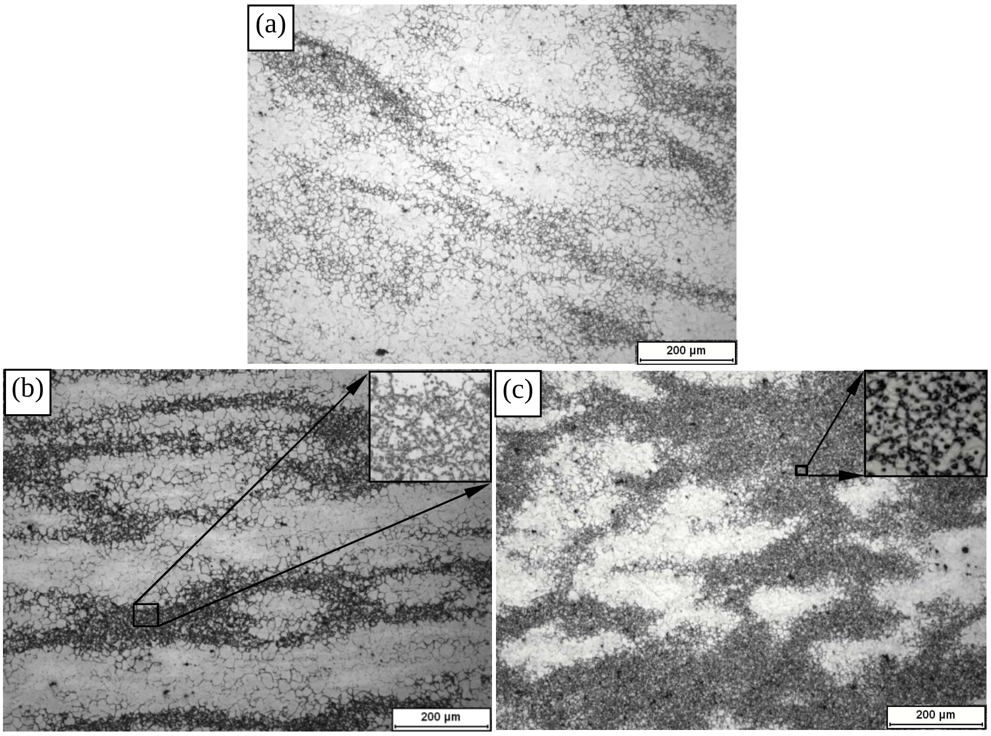

Fig. 4 Micro-structure of the MDF samples, (a) P1-sample, (B) P2-sample. (c) P3-sample

During the MDF process, the precipitation of $Mg_{17}Al_{12}$ phase should be related with the deforming temperature, accumulative strains and Al content in local position. The deforming temperature and the accumulative strains are probably consistent on the local micro region with or without $Mg_{17}Al_{12}$ phase. So the precipitation of $Mg_{17}Al_{12}$ phase should be mainly controlled by the Al content in the Mg matrix. As aforementioned, the solute distribution in the initial alloy is inhomogenous, which will naturally result in an ununiform precipitation of the $Mg_{17}Al_{12}$ phase. This has also been proved by the above-mentioned EPMA measurement. As a consequence, fine and coarse grains coexist in the microstructures.

Difference from the static aging precipitation, the precipitation of $Mg_{17}Al_{12}$ phase during the MDF process is be accompanied by constantly increasing the accumulative strain and dynamic recrystallization. Under the interaction among the strain, recrystallization and precipitation, the $Mg_{17}Al_{12}$ phase precipitate from the Mg matrix and formed granular shape. These granular $Mg_{17}Al_{12}$ phases can refine the grain of AZ80 alloys by pin up the grain boundaries. With the decreasing of forging temperature, more $Mg_{17}Al_{12}$ phase precipitate from the Mg matrix and the area of fine grains expanded, as shown in Fig. 4

4. Conclusions

(1) The β- $Mg_{17}Al_{12}$ phases with granular shape unevenly precipitated from the Mg matrix, as AZ80 Mg alloy multi-directional forged with decreasing temperature from 410 to 300 ℃. These $Mg_{17}Al_{12}$ phase retards the growth of the DRX grains, which in turns results in the formation fine grains area.

(2) With increasing the accumulative strains and decreasing temperature, the fine grains area with granular $Mg_{17}Al_{12}$ phase expanded.

(3) The EPMA analysis show that the inhomogenous Al content distribution in the Mg matrix leads to the non-uniform dynamic precipitation of the $Mg_{17}Al_{12}$ phase.

5. Acknowledgement
This work was supported by the National Natural Science Foundation of China (Nos. 51204053, 51674078 and 51374067), the Fundamental Research Fund for Central Universitis (Nos. N160913002， N130409005 and N130209001) and A Project supported by Scientific Research Fund of Liaoning Province (No. 2015022003).

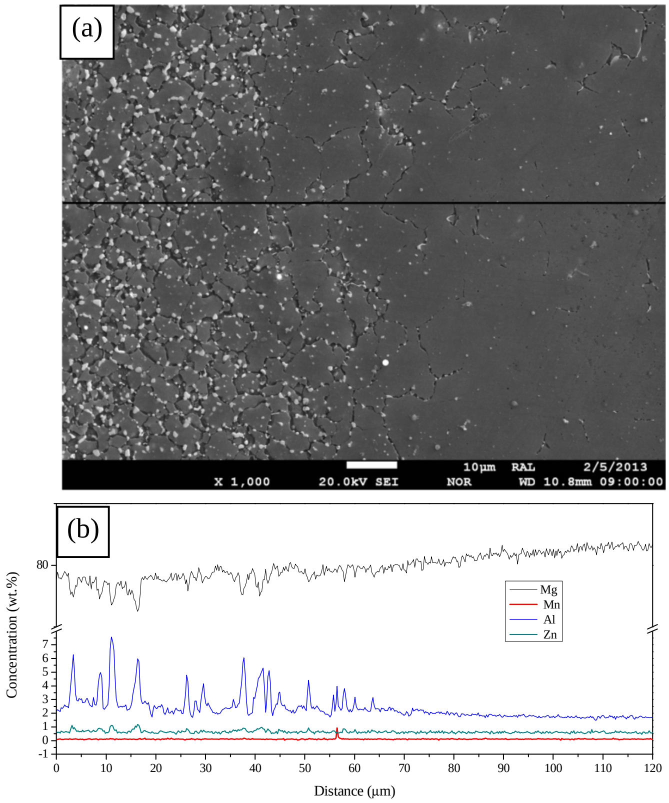

Fig.5 Microprobe measurements of Mg, Mn Zn and Al concentrations in the coarse and fine grain regions of P3-sample, (a) the SEM photo in the intersection area of coarse and fine grain (b) the distribution of the elements along the scanning line in (a).

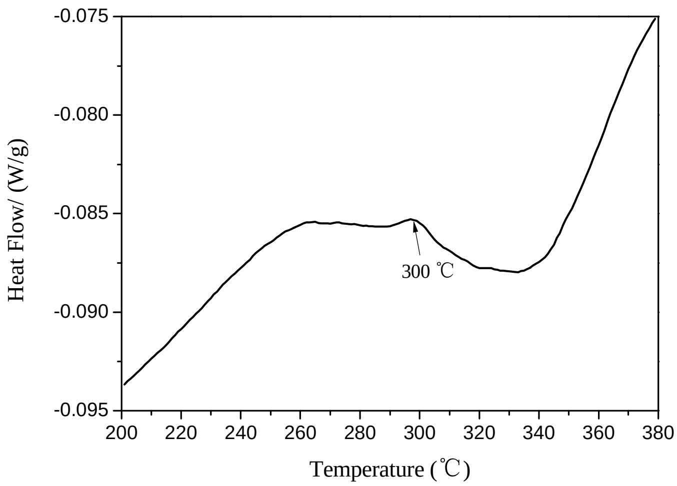

Fig. 6 Typical DSC scan at a heating rate of 5 ℃/min of the as casting AZ80

IOP Conf. Series: Materials Science and Engineering **194** (2017) 012015 doi:10.1088/1757-899X/194/1/012015

References

[1] Ha J.S. and Hong S I. 2016. *Materials Science and Engineering: A.*, **651** 805.
[2] Choudhary B.K. Samuel E.I. Sainath G, et al. 2013. *Metallurgical and Materials Transactions A.* **44** 4979.
[3] Nagesha A, Kannan R, Srinivasan V. S., et al. 2016. *Metallurgical and Materials Transactions A.* **47** 1110
[4] Araujo J., Gabriel S., Dille J. et al. 2015. *Journal of alloys and compounds.* **43(S1)** S256
[5] Aboulfadl H, Deges J, Choi P. et al. 2015 *Acta Materialia.* **86** 1110
[6] Zhilyaev A.P. Shakhova I. Morozova A. et al. 2016 *Materials Science and Engineering: A.*, **654** 131
[7] Roven H., Liu M., Werenskiold J. 2008. *Materials Science and Engineering: A.* **483** 54
[8] Zha M., Li Y., Mathiesen R. et al. 2015. *Acta Materialia,* **84** 42.
[9] Xia X., Chen Q., Zhao Z., et al. 2015. *Journal of Alloys and Compounds.* **623** 62.
[10] Nie K., Wang X., Ddeng. K., et al. 2015. *Journal of Alloys and Compounds*, **617** 979
[11] Jiang M., Yan H., Chen R. 2015. *Journal of Alloys and Compounds,* **650** 399
[12] Zhu Q.F., Li L., Zhang Z.Q. et. al. 2014. *Materials Transactions,* **55** 270